Atmospheric Environment: X 2 (2019) 100019

Contents lists available at ScienceDirect

Atmospheric Environment: X

journal homepage: www.journals.elsevier.com/atmospheric-environment-x

A system for developing and projecting $PM_{2.5}$ spatial fields to correspond to just meeting national ambient air quality standards

James T. Kelly[a,*], Carey J. Jang[a], Brian Timin[a], Brett Gantt[a], Adam Reff[a], Yun Zhu[b], Shicheng Long[b], Adel Hanna[c]

[a] Office of Air Quality Planning and Standards, U.S. Environmental Protection Agency, Research Triangle Park, NC, USA
[b] College of Environment and Energy, South China University of Technology, Guangzhou Higher Education Mega Center, Guangzhou, China
[c] Institute for the Environment, University of North Carolina at Chapel Hill, NC, 27517, USA

ARTICLE INFO

Keywords:
Air quality modeling
$PM_{2.5}$ projection
Cross validation
Spatial prediction model

ABSTRACT

$PM_{2.5}$ concentration fields that correspond to just meeting national ambient air quality standards (NAAQS) are useful for characterizing exposure in regulatory assessments. Computationally efficient methods that incorporate predictions from photochemical grid models (PGMs) are needed to realistically project baseline concentration fields for these assessments. Thorough cross validation (CV) of hybrid spatial prediction models is also needed to better assess their predictive capability in sparsely monitored areas. In this study, a system for generating, evaluating, and projecting $PM_{2.5}$ spatial fields to correspond with just meeting the $PM_{2.5}$ NAAQS is developed and demonstrated. Results of ten-fold CV based on standard and spatial cluster withholding approaches indicate that performance of three spatial prediction models improves with decreasing distance to the nearest neighboring monitor, improved PGM performance, and increasing distance from sources of $PM_{2.5}$ heterogeneity (e.g., complex terrain and fire). An air quality projection tool developed here is demonstrated to be effective for quickly projecting $PM_{2.5}$ spatial fields to just meet NAAQS using realistic spatial response patterns based on air quality modeling. $PM_{2.5}$ tends to be most responsive to primary $PM_{2.5}$ emissions in urban areas, whereas response patterns are relatively smooth for NOx and SO_2 emission changes. On average, $PM_{2.5}$ is more responsive to changes in anthropogenic primary $PM_{2.5}$ emissions than NOx and SO_2 emissions in the contiguous U.S.

1. Introduction

The U.S. air quality management system is a cyclical process driven by the goals of meeting national ambient air quality standards (NAAQS) (Bachmann, 2007; NRC, 2004). NAAQS are set by the U.S. Environmental Protection Agency (EPA) for six criteria pollutants, including fine particulate matter ($PM_{2.5}$), to protect public health and welfare. Air quality concentrations are projected to levels that just meet NAAQS as part of risk and exposures assessments (REAs) often conducted during NAAQS reviews. Specifically, air quality concentrations are projected such that the highest monitored design value (DV; www.epa.gov/air-trends/air-quality-design-values) in the area equals (i.e., just meets) the NAAQS. REA analyses can consider many areas across the U.S. and potential alternative NAAQS levels in addition to existing standards (e.g., USEPA, 2010; USEPA, 2014). Projecting air quality to just meet NAAQS for many scenarios is challenging due to the computational expense of the photochemical grid models (PGMs) commonly used for air quality projection.

In a previous study (Kelly et al., 2017), we described a method to quickly project monitored $PM_{2.5}$ concentrations to levels that correspond to just meeting NAAQS. Strengths of the method include fast application for multiple NAAQS in areas throughout the U.S., consistency with EPA guidelines for projecting $PM_{2.5}$ DVs in regulatory assessments (USEPA, 2007), and the option to project DVs according to multiple emission scenarios. A limitation of the method is that the $PM_{2.5}$ response factors were based on simulations with emission decreases only, whereas simulations for both emission decreases and increases would facilitate broader application. The method also neglects nonlinear interactions in chemistry when applied for combinations of emission reduction cases. Furthermore, the approach projects $PM_{2.5}$ at monitoring sites, but the epidemiologic studies that inform health impact assessments are increasingly based on spatial concentration fields rather than concentrations at discrete monitoring sites (e.g., Crouse et al., 2015; Di et al., 2017a; Di et al., 2017b; Shi et al., 2016).

* Corresponding author. Air Quality Modeling Group, Air Quality Assessment Division, Office of Air Quality Planning & Standards, Office of Air & Radiation, US Environmental Protection Agency, 109 TW Alexander Drive, Mail Drop: C439-01, Research Triangle Park, NC, 27711, USA.
E-mail address: kelly.james@epa.gov (J.T. Kelly).

https://doi.org/10.1016/j.aeaoa.2019.100019
Received 8 November 2018; Received in revised form 28 January 2019; Accepted 3 February 2019
Available online 12 February 2019

Many hybrid methods have been developed in recent years to create $PM_{2.5}$ spatial fields by combining information from monitoring and other sources such as air quality models, satellites, and land-use data (e.g., Beckerman et al., 2013; Berrocal et al., 2012; Di et al., 2016; Friberg et al., 2016; Hu et al., 2017; Keller et al., 2015; Kim et al., 2017; Kloog et al., 2014; Lv et al., 2016; van Donkelaar et al., 2015; Wang et al., 2016; Wang et al., 2018). Predictions from these methods agree reasonably well with withheld observations in cross validation (CV) assessments. However, typical CV withholding approaches may overestimate predictive capability in areas with limited or no monitors (Huang et al., 2018). Recently, a Data Fusion Tool (DFT) was developed to facilitate the creation and evaluation of spatial concentration fields (Li et al., 2019; www.abacas-dss.com/abacas/Software.aspx). DFT currently develops spatial fields according to three methods: Voronoi neighbor averaging (VNA), enhanced-VNA (eVNA), and the downscaler approach of Berrocal et al. (2012). However, DFT versions applied to date do not enable the spatial cluster withholding approaches recommended in recent studies to thoroughly assess the predictive capability of spatial prediction models (Huang et al., 2018; Lv et al., 2016; Young et al., 2016).

In this study, a system for generating, evaluating, and projecting $PM_{2.5}$ spatial fields to correspond with just meeting $PM_{2.5}$ NAAQS is developed and demonstrated. DFT is applied to predict gridded $PM_{2.5}$ concentration fields according to three methods and evaluate predictions using CV based on standard and spatial cluster withholding approaches. The method of Kelly et al. (2017) is updated to enable projection of $PM_{2.5}$ spatial fields in addition to monitored concentrations. The system is then demonstrated for a case study in the Houston-The Woodlands-Sugar Land core based statistical area (CBSA) in Texas.

2. Methods

The system for projecting $PM_{2.5}$ spatial fields to correspond to just meeting NAAQS for air quality and health impact assessments is shown in Fig. 1. First, total and speciated $PM_{2.5}$ data are acquired from the air quality system (AQS) database of measurements from U.S. air quality networks (www.epa.gov/aqs). $PM_{2.5}$ concentrations are also simulated for 2015 baseline and emission sensitivity cases using the Community Multiscale Air Quality (CMAQ; www.epa.gov/cmaq) model to provide a national modeled field of $PM_{2.5}$ and estimates of how the field would respond to changes in emissions. Sensitivity simulations were conducted for percent changes in U.S. anthropogenic emissions of NOx and SO_2 of −100%, −75%, −50%, −25%, +25%, +50%, and +75% and percent changes in U.S. anthropogenic primary $PM_{2.5}$ emissions of −50% and +50%. The suite of sensitivity simulations developed here are similar to those of Kelly et al. (2017) but include cases with emission increases and are relative to a baseline simulation for 2015 rather than 2011. More details on the CMAQ modeling are provided in the Supplementary Information, Section S1.

Second, DFT predicts daily average $PM_{2.5}$ concentrations on a spatial grid covering the contiguous U.S. according to three methods (VNA, eVNA, and downscaler) using $PM_{2.5}$ concentrations from monitors and the 2015 baseline CMAQ simulation. The VNA method interpolates monitored concentrations to a spatial grid using inverse-distance-squared weighted averaging of monitored concentrations in neighboring Voronoi polygons. The eVNA method applies VNA interpolation to monitored concentrations that have been scaled by the ratio of the CMAQ concentration in the grid cell containing the prediction point to the CMAQ concentration in the grid cell containing the monitor (Fann et al., 2018). The downscaler approach is a Bayesian statistical model that regresses CMAQ predictions on monitor data and uses the resulting relationships to predict $PM_{2.5}$ based on a CMAQ input field (Berrocal et al., 2012; USEPA, 2017).

Relative response factors (RRFs; USEPA, 2007) are used to project $PM_{2.5}$ concentrations at monitor locations and on the spatial grid. RRFs are calculated using predictions from the baseline and emission-sensitivity CMAQ simulations with the Software for Model Attainment Test-Community Edition (SMAT-CE; www.epa.gov/scram/photochemical-modeling-tools). RRFs for $PM_{2.5}$ components are calculated as the ratio of the component concentration in the sensitivity simulation to that in the baseline simulation. Total $PM_{2.5}$ RRFs are then calculated as the weighted average of the component RRFs using speciated concentrations based on observations as weighting factors (Kelly et al., 2017). This step results in $PM_{2.5}$ RRFs for each emission sensitivity case at each monitor and on the spatial grid. The $PM_{2.5}$ RRFs corresponding to the simulated emission sensitivity cases are then interpolated across the range of emission changes from −100 to 100% for each emission scenario.

Third, the interpolated $PM_{2.5}$ RRFs, $PM_{2.5}$ concentrations at monitors, and the baseline $PM_{2.5}$ spatial field are input to the air quality projection tool (APT) developed here. APT iterates over projections of $PM_{2.5}$ DVs at monitors in the selected area using RRFs corresponding to

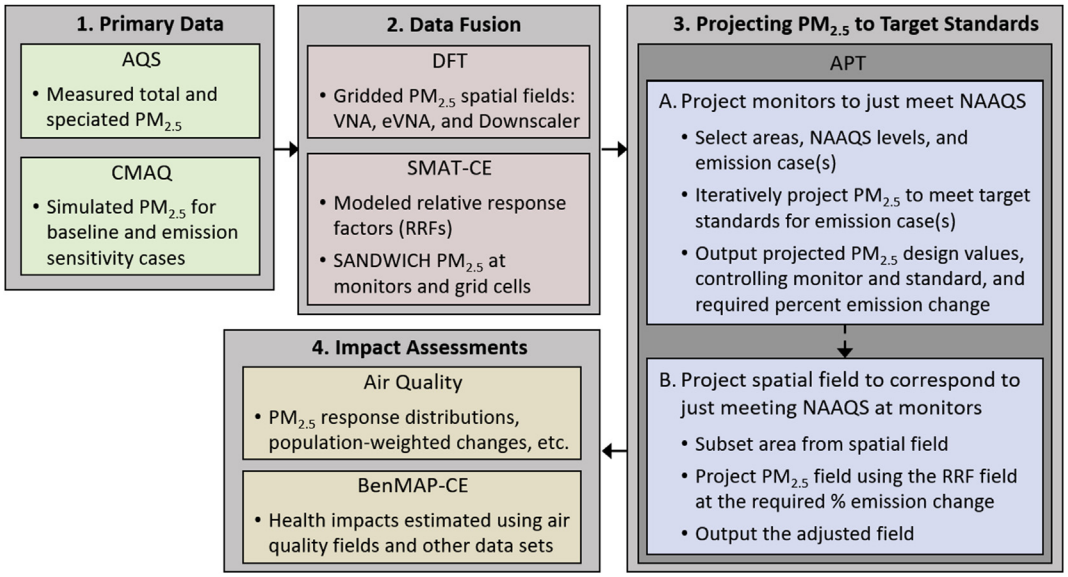

Fig. 1. Overview of system for projecting $PM_{2.5}$ spatial fields to correspond to just meeting NAAQS. SANDWICH: Sulfate, Adjusted Nitrate, Derived Water, Inferred Carbonaceous material balance approach (Frank, 2006).

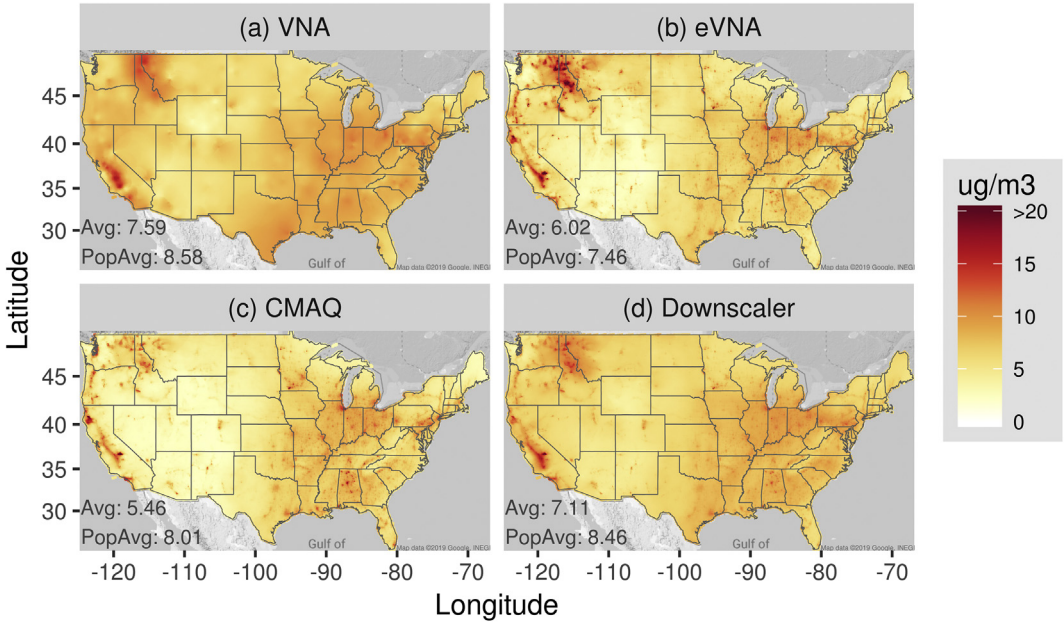

Fig. 2. Predictions of 2015 annual average $PM_{2.5}$ over the contiguous U.S. based on (a) VNA, (b) eVNA, (c) CMAQ, and (d) downscaler. Avg and PopAvg indicate the average and population-weighted average $PM_{2.5}$ in $\mu g\ m^{-3}$, respectively.

different emission reduction levels until the target combination of 24-hr and annual standards is just met (i.e., the highest $PM_{2.5}$ DV in the area equals the standard). This step identifies the percent emission reduction required to just meet the NAAQS at the controlling monitor (i.e., the monitor requiring the greatest percent emission reduction). The portion of the $PM_{2.5}$ spatial field overlapping the selected area is then extracted from the national field and is projected using the spatial field of RRFs corresponding to the percent emission reduction needed for the monitors in the area to just meet the NAAQS.

Finally, the baseline and projected $PM_{2.5}$ spatial fields are input into downstream programs for air quality impact assessment or potentially the Environmental Benefits Mapping and Analysis Program – Community Edition (BenMAP-CE; Sacks et al., 2018) for health impact assessment.

3. Results and discussion

3.1. $PM_{2.5}$ spatial fields and cross validation (CV)

Annual average $PM_{2.5}$ concentrations over the contiguous U.S. predicted by VNA, eVNA, CMAQ, and downscaler for 2015 are shown in Fig. 2. The VNA spatial field is relatively smooth and has greater average $PM_{2.5}$ ($7.59\ \mu g\ m^{-3}$) than the other methods ($5.46–7.11\ \mu g\ m^{-3}$) due to interpolation of relatively high concentrations observed in urban areas to surrounding areas. Population-weighted average $PM_{2.5}$ based on VNA ($8.58\ \mu g\ m^{-3}$) is similar to that based on downscaler ($8.46\ \mu g\ m^{-3}$) suggesting that VNA and downscaler predict similar concentrations in urban areas. The difference between the average and population-weighted average concentration is greatest for the CMAQ field due to relatively sharp gradients between urban and surrounding areas. Due to the influence of these gradients on the eVNA interpolation of monitored concentrations, the average and population-weighted average concentrations for eVNA are lower than for VNA and downscaler (Fig. 2).

Predictions of VNA, eVNA, and downscaler were evaluated using ten-fold CV as follows. The monitoring sites were first divided into ten subsets or "folds." One fold (10% of the monitors) was then withheld in the VNA and eVNA interpolations and the fitting of the downscaler model, and $PM_{2.5}$ predictions were made at the locations of the withheld monitors using each method. These steps were then repeated for the other nine folds to yield a CV prediction from each method at each site. Regional R^2 based on this approach ranges from 0.35 (Northwest) to 0.82 (Upper Midwest) for downscaler, 0.51 (Northwest) to 0.84 (Upper Midwest) for VNA, and 0.18 (Northwest) to 0.74 (Ohio Valley) for eVNA (Table S2).

The spatial prediction models performed relatively well in regions where CMAQ performed well. For instance, R^2 for CMAQ predictions is 0.20 in the Northwest, where CV R^2 ranges from 0.18 to 0.51, and is 0.42 in the Upper Midwest, where CV R^2 ranges from 0.73 to 0.84. Regional performance for the spatial prediction models is strongly correlated with performance for CMAQ (r: 0.6–0.8; Fig. S4). The spatial prediction models also performed relatively well in regions where sources of $PM_{2.5}$ heterogeneity are limited. For instance, R^2 is frequently low for sites in the western U.S. where terrain is complex and wildfire emissions strongly influence $PM_{2.5}$ concentrations (Fig. S2). Previous studies have also reported challenges in modeling $PM_{2.5}$ in the western U.S. for these reasons (Di et al., 2016; Geng et al., 2018; Hu et al., 2017; Wang et al., 2018). Finally, the spatial prediction models performed well in areas where monitor siting is dense. For instance, the average R^2 is 0.78 for the downscaler method for sites within 22 km of another site and is 0.67 for sites whose nearest neighbor is farther than 22 km (i.e., the median nearest-neighbor distance). The higher density of monitors in areas with higher $PM_{2.5}$ concentrations explains in part the trend of increasing R^2 with increasing observed $PM_{2.5}$ concentration (Fig. S3).

To further investigate the influence of monitoring density on CV results, ten-fold CV was repeated for January and July for cases where monitors within a specified radius of the primary withheld monitor were also withheld. In Fig. 3, national total R^2 based on predictions at the primary withheld monitors is shown as a function of the withholding radius. As the radius increases from 0 to 50 km, the number of in-sample monitors decreases from 938 (90% of available monitors) to 628 (60% of available monitors), and total R^2 decreases for all methods. For example, total R^2 for downscaler decreases from 0.65 to 0.47 in January as the withholding radius increases from 0 to 50 km. These results demonstrate that favorable statistics for densely monitored areas do not necessarily imply favorable performance in more sparsely monitored parts of the domain.

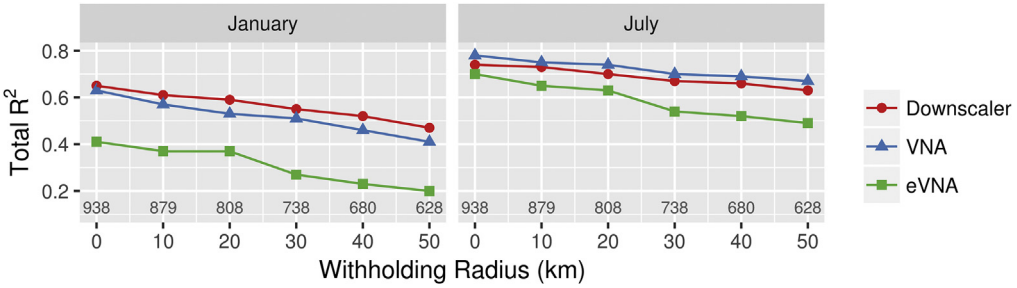

Fig. 3. Total R^2 for downscaler, VNA, and eVNA as a function of withholding radius for January and July 2015 (grey text indicates the number of in-sample monitors).

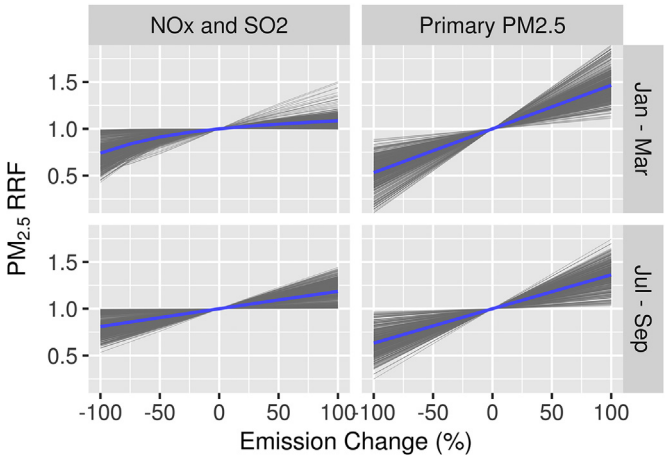

Fig. 4. $PM_{2.5}$ RRFs at U.S. monitoring sites for changes in anthropogenic primary $PM_{2.5}$ and NOx and SO_2 emissions during the first and third quarters of 2015. Grey lines indicate individual sites; blue lines indicate mean. (For interpretation of the references to colour in this figure legend, the reader is referred to the web version of this article.)

3.2. $PM_{2.5}$ RRFs

$PM_{2.5}$ RRFs corresponding to the two emission cases are shown in Fig. 4 for the first and third quarters of 2015 at 672 sites. $PM_{2.5}$ observations and spatial fields are projected by multiplication with $PM_{2.5}$ RRFs (e.g., RRFs less than one result in lower projected $PM_{2.5}$ than baseline $PM_{2.5}$). For the NOx and SO_2 case, there is curvature in the RRF-emission change relationship during January through March due to the influence of chemical feedbacks of NOx on sulfate and nitrate production under conditions of low photochemical activity in winter (e.g., Pusede et al., 2016; Shah et al., 2018). During July through September, the RRF-emission change relationship is approximately linear and indicates a roughly 9% change in $PM_{2.5}$ for a 50% change in NOx and SO_2 emissions on average. For primary $PM_{2.5}$ emission changes, the RRF-emission change relationship is approximately linear in both quarters and indicates a roughly 18% change in $PM_{2.5}$ for a 50% change in emissions on average during July through September.

Spatial fields of annual average $PM_{2.5}$ RRFs for 50% reductions in emissions of primary $PM_{2.5}$ and NOx and SO_2 are shown in Fig. 5. NOx and SO_2 emission reductions result in $PM_{2.5}$ RRFs less than about 0.9 in broad areas of the eastern U.S. and California where $PM_{2.5}$ sulfate and nitrate concentrations are elevated (e.g., Hand et al., 2012). The average $PM_{2.5}$ RRF (0.93) is close to the population-weighted average RRF (0.92) for the NOx and SO_2 case due to the spatially smooth response of secondary $PM_{2.5}$ to precursor emission reductions. In contrast, the average $PM_{2.5}$ RRF for the primary $PM_{2.5}$ emission case (0.86) is higher than the population-weighted average RRF (0.80) indicating that $PM_{2.5}$ is relatively responsive to primary $PM_{2.5}$ emission reductions in populated areas. Overall, anthropogenic primary $PM_{2.5}$ emission reductions have a larger influence on $PM_{2.5}$ in urban than rural areas and a greater influence on average than the same percent reduction in NOx and SO_2 emissions (Fig. 5).

3.3. Case study: Houston-The Woodlands-Sugar Land, Texas

In this section, the projection approach described above is illustrated for a case study in Houston, Texas for the existing levels of the annual (12 $\mu g\,m^{-3}$) and 24-hr (35 $\mu g\,m^{-3}$) $PM_{2.5}$ NAAQS. The Houston case study was selected because the $PM_{2.5}$ spatial response patterns for Houston are common to many of the urban areas we examined in the U.S. As in Kelly et al. (2017), the PGM-based projections are compared with projections of a statistical approach known as the proportional method that has been used in previous NAAQS reviews. In the proportional method, the spatial field is uniformly scaled by a fixed percentage that corresponds to the percent difference between the highest $PM_{2.5}$ DV in the area and the NAAQS level. For brevity, results are presented below for projections of the downscaler field; results for projections of the VNA and eVNA fields are provided in the supplementary information.

In the nine counties that comprise the Houston-The Woodlands-Sugar Land CBSA, the highest 2014–2016 annual $PM_{2.5}$ DV is 11.2 $\mu g\,m^{-3}$ and the highest 24-hr $PM_{2.5}$ DV is 22 $\mu g\,m^{-3}$ both in Harris County. Compared with existing NAAQS levels, the highest annual DV is 7% below the annual NAAQS level and the highest 24-hr DV is 59% below the 24-hr NAAQS level. The percent change in the downscaler $PM_{2.5}$ field associated with projecting DVs in the CBSA to just meet the NAAQS is shown in Fig. 6 for four cases: (a) proportional, (b) primary $PM_{2.5}$ emission changes, (c) NOx and SO_2 emission changes, and (d) elimination of 50% of the difference between DVs and the NAAQS level with NOx and SO_2 emission changes and 50% with primary $PM_{2.5}$ emission changes (i.e., 'Combined' in Fig. 6). The proportional method uniformly projects $PM_{2.5}$ in each grid cell by the greatest percent difference between the $PM_{2.5}$ DVs and the NAAQS (i.e., −7%). In the primary $PM_{2.5}$ projection case, grid cells near the controlling monitor are also projected to concentrations about 7% higher than baseline concentrations, but smaller absolute percent changes occur in surrounding grid cells. This pattern results from the relatively high responsiveness of $PM_{2.5}$ to primary $PM_{2.5}$ emission changes in central Houston compared with the outlying areas. For the NOx and SO_2 projection case, the opposite behavior occurs (i.e., $PM_{2.5}$ concentrations in the outlying cells increase by greater than the 7% increase required at the controlling monitor in central Houston). The relatively low responsiveness of $PM_{2.5}$ in central Houston to NOx and SO_2 emission changes is consistent with the location of important SO_2 sources outside of the urban core and chemical feedbacks of NOx changes on HOx precursors (e.g., Pusede et al., 2016). The $PM_{2.5}$ response pattern for the combined emission case is similar to that of the proportional method due to the superposition of opposite response patterns for the primary $PM_{2.5}$ and NOx and SO_2 emission cases (Fig. 6).

Average and population-weighted average changes in $PM_{2.5}$ concentration ($\Delta PM_{2.5}$) are provided in Table 1 for projection of the

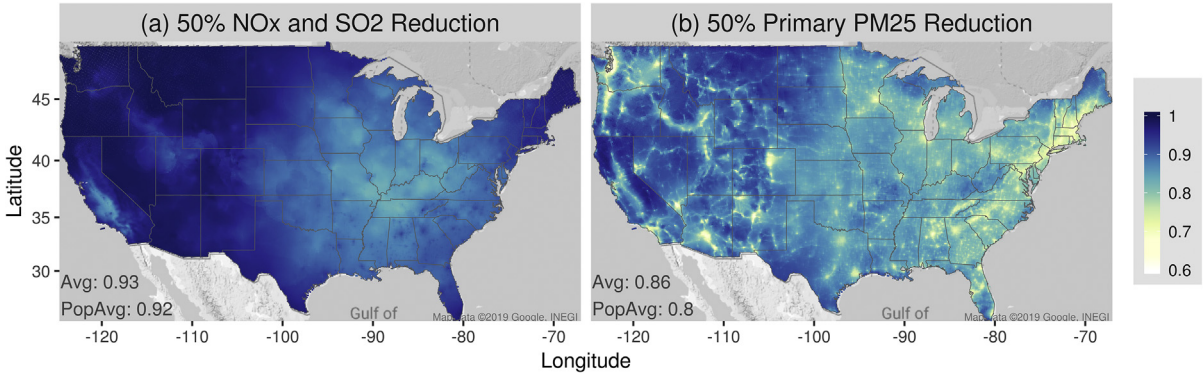

Fig. 5. $PM_{2.5}$ RRFs for 50% reductions in U.S. anthropogenic (a) NOx and SO_2 and (b) primary $PM_{2.5}$ emissions. Text indicates average and population-weighted average values.

downscaler field for the four cases in the Houston example. Average $\Delta PM_{2.5}$ ranged from 0.49 $\mu g\,m^{-3}$ for the primary $PM_{2.5}$ case to 1.05 $\mu g\,m^{-3}$ for the NOx and SO_2 case. Population-weighted average $\Delta PM_{2.5}$ ranged from 0.61 $\mu g\,m^{-3}$ for the primary $PM_{2.5}$ case to 1.08 $\mu g\,m^{-3}$ for the NOx and SO_2 case. The relatively large difference between the average and population-weighted average $\Delta PM_{2.5}$ for the primary $PM_{2.5}$ emission case is driven by the relatively high sensitivity of $PM_{2.5}$ concentrations to primary $PM_{2.5}$ emissions in the most populous county in the CBSA (Harris). For the combined emission and proportional projection cases, average $\Delta PM_{2.5}$ values are between the relatively low value for the primary $PM_{2.5}$ case and high value for the NOx and SO_2 case and are similar in magnitude (i.e., 0.73 $\mu g\,m^{-3}$ for the combined emission case and 0.71 $\mu g\,m^{-3}$ for the proportional method). The average $\Delta PM_{2.5}$ values for projection of the downscaler field were between values for projection of the eVNA and VNA fields (Table S3). Projecting fields based on multiple approaches provides flexibility for characterizing the sensitivity of health impacts to different air quality scenarios or using the most suitable approach for a given application.

4. Summary and conclusions

A system for generating, evaluating, and projecting $PM_{2.5}$ spatial fields to correspond with just meeting $PM_{2.5}$ NAAQS is developed and demonstrated. In ten-fold CV tests, regional R^2 ranges from 0.35 to 0.82 for downscaler, 0.51 to 0.84 for VNA, and 0.18 to 0.74 for eVNA. CV results based on standard and spatial cluster withholding approaches indicate that performance of the methods improves with decreasing distance to the nearest neighboring monitor, improved PGM performance, and increasing distance from sources of $PM_{2.5}$ heterogeneity (e.g., complex terrain and fire). Performance also tends to be better for sites with higher observed concentrations, possibly due to the higher density of monitors in areas with relatively high $PM_{2.5}$ concentration. The APT projection tool developed here is found to be effective for quickly projecting $PM_{2.5}$ fields according to realistic spatial response

Table 1
Summary of results for the Houston case study.

Projection Case	ΔEmission Primary $PM_{2.5}$ (%)	ΔEmission NOx and SO_2 (%)	Average $\Delta PM_{2.5}$ ($\mu g\,m^{-3}$)	Pop. Wt. Avg. $\Delta PM_{2.5}$ ($\mu g\,m^{-3}$)
Primary $PM_{2.5}$	14	0	0.49	0.61
NOx and SO_2	0	92	1.05	1.08
Combined	6	44	0.73	0.81
Proportional	N/A	N/A	0.71	0.77

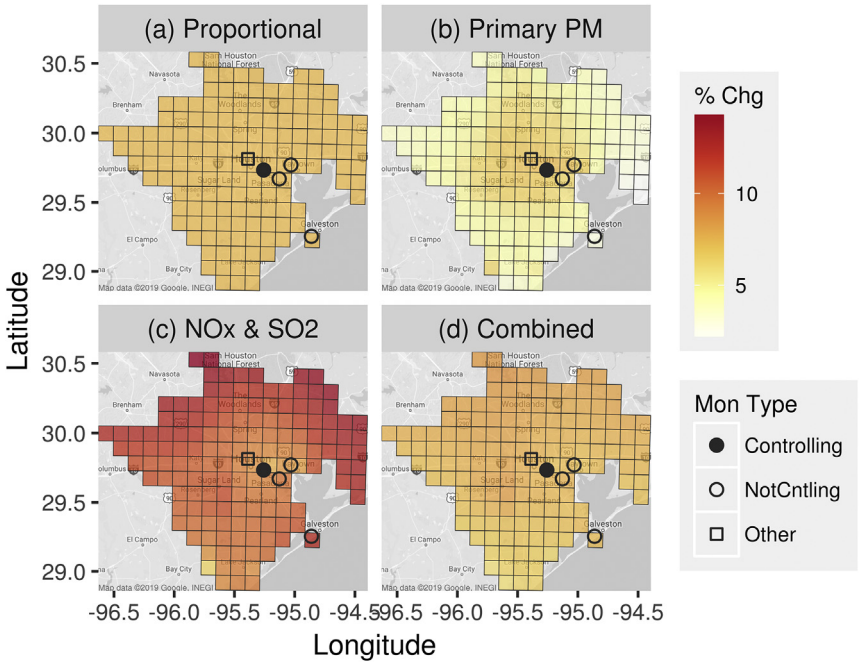

Fig. 6. Percent change in 2015 annual average $PM_{2.5}$ (downscaler) associated with projecting 2014–2016 DVs at monitors to just meet NAAQS according to four spatial response patterns for counties in the Houston area. 'Other' indicates a monitor that was used in developing the spatial field but not in projecting 2014–2016 DVs, because this monitor began sampling in 2015.

patterns based on air quality modeling for multiple emission cases. $PM_{2.5}$ tends to be most responsive to primary $PM_{2.5}$ emissions in urban areas, whereas response patterns are relatively smooth for NOx and SO_2 emission changes. On average, $PM_{2.5}$ is more responsive to changes in anthropogenic primary $PM_{2.5}$ emissions than NOx and SO_2 emissions in the contiguous U.S.

Disclaimer

The views in this manuscript are those of the authors alone and do not necessarily reflect the policy of the U.S. Environmental Protection Agency.

Declaration of interests

None.

Acknowledgments

The authors thank Drs. Kristen Foley and Jennifer Richmond-Bryant for helpful comments on an early draft of this article.

Appendix A. Supplementary data

Supplementary data to this article can be found online at https://doi.org/10.1016/j.aeaoa.2019.100019.

References

Bachmann, J., 2007. Will the circle be unbroken: a history of the US national ambient air quality standards. J. Air Waste Manag. Assoc. 57, 652–697.
Beckerman, B.S., Jerrett, M., Serre, M., Martin, R.V., Lee, S.J., van Donkelaar, A., Ross, Z., Su, J., Burnett, R.T., 2013. A hybrid approach to estimating national scale spatiotemporal variability of PM2.5 in the contiguous United States. Environ. Sci. Technol. 47, 7233–7241.
Berrocal, V.J., Gelfand, A.E., Holland, D.M., 2012. Space-time data fusion under error in computer model output: an application to modeling air quality. Biometrics 68, 837–848.
Crouse, D.L., Peters, P.A., Hystad, P., Brook, J.R., van Donkelaar, A., Martin, R.V., Villeneuve, P.J., Jerrett, M., Goldberg, M.S., Pope, C.A., Brauer, M., Brook, R.D., Robichaud, A., Menard, R., Burnett, R.T., 2015. Ambient PM2.5, O3, and NO2 exposures and associations with mortality over 16 Years of follow-up in the Canadian census health and environment cohort (CanCHEC). Environ. Health Perspect. 123, 1180–1186.
Di, Q., Dai, L., Wang, Y., et al., 2017a. Association of short-term exposure to air pollution with mortality in older adults. J. Am. Med. Assoc. 318, 2446–2456.
Di, Q., Kloog, I., Koutrakis, P., Lyapustin, A., Wang, Y.J., Schwartz, J., 2016. Assessing PM2.5 exposures with high spatiotemporal resolution across the continental United States. Environ. Sci. Technol. 50, 4712–4721.
Di, Q., Wang, Y., Zanobetti, A., Wang, Y., Koutrakis, P., Choirat, C., Dominici, F., Schwartz, J.D., 2017b. Air pollution and mortality in the medicare population. N. Engl. J. Med. 376, 2513–2522.
Fann, N., Coffman, E., Timin, B., Kelly, J.T., 2018. The estimated change in the level and distribution of PM2.5-attributable health impacts in the United States: 2005–2014. Environ. Res. 167, 506–514.
Frank, N.H., 2006. Retained nitrate, hydrated sulfates, and carbonaceous mass in Federal Reference Method fine particulate matter for six eastern US cities. J. Air Waste Manag. Assoc. 56, 500–511.
Friberg, M.D., Zhai, X.X., Holmes, H.A., Chang, H.H., Strickland, M.J., Sarnat, S.E., Tolbert, P.E., Russell, A.G., Mulholland, J.A., 2016. Method for fusing observational data and chemical transport model simulations to estimate spatiotemporally resolved ambient air pollution. Environ. Sci. Technol. 50, 3695–3705.
Geng, G., Murray, N.L., Tong, D., Fu, J.S., Hu, X., Lee, P., Meng, X., Chang, H.H., Liu, Y., 2018. Satellite-based daily PM2.5 estimates during fire seasons in Colorado. J. Geophys. Res. Atmosphere 123, 8159–8171.
Hand, J.L., Schichtel, B.A., Pitchford, M., Malm, W.C., Frank, N.H., 2012. Seasonal composition of remote and urban fine particulate matter in the United States. J. Geophys. Res.: Atmosphere 117.
Hu, X., Belle, J.H., Meng, X., Wildani, A., Waller, L.A., Strickland, M.J., Liu, Y., 2017. Estimating PM2.5 concentrations in the conterminous United States using the random forest approach. Environ. Sci. Technol. 51, 6936–6944.
Huang, R., Zhai, X., Ivey, C.E., Friberg, M.D., Hu, X., Liu, Y., Di, Q., Schwartz, J., Mulholland, J.A., Russell, A.G., 2018. Air pollutant exposure field modeling using air quality model-data fusion methods and comparison with satellite AOD-derived fields: application over North Carolina, USA. Air Qual. Atmos. Health 11, 11–22.
Keller, J.P., Olives, C., Kim, S.Y., Sheppard, L., Sampson, P.D., Szpiro, A.A., Oron, A.P., Lindstrom, J., Vedal, S., Kaufman, J.D., 2015. A unified spatiotemporal modeling approach for predicting concentrations of multiple air pollutants in the multi-ethnic study of atherosclerosis and air pollution. Environ. Health Perspect. 123, 301–309.
Kelly, J.T., Reff, A., Gantt, B., 2017. A method to predict PM2.5 resulting from compliance with national ambient air quality standards. Atmos. Environ. 162, 1–10.
Kim, S.Y., Olives, C., Sheppard, L., Sampson, P.D., Larson, T.V., Keller, J.P., Kaufman, J.D., 2017. Historical prediction modeling approach for estimating long-term concentrations of PM2.5 in cohort studies before the 1999 implementation of widespread monitoring. Environ. Health Perspect. 125, 38–46.
Kloog, I., Chudnovsky, A.A., Just, A.C., Nordio, F., Koutrakis, P., Coull, B.A., Lyapustin, A., Wang, Y.J., Schwartz, J., 2014. A new hybrid spatio-temporal model for estimating daily multi-year PM2.5 concentrations across northeastern USA using high resolution aerosol optical depth data. Atmos. Environ. 95, 581–590.
Li, J., Zhu, Y., Kelly, J.T., Jang, C.J., Wang, S., Hanna, A., Xing, J., Lin, C.-J., Long, S., Yu, L., 2019. Health benefit assessment of PM2.5 reduction in Pearl River Delta region of China using a model-monitor data fusion approach. J. Environ. Manag. 233, 489–498.
Lv, B.L., Hu, Y.T., Chang, H.H., Russell, A.G., Bai, Y.Q., 2016. Improving the accuracy of daily PM2.5 distributions derived from the fusion of ground-level measurements with aerosol optical depth observations, a case study in North China. Environ. Sci. Technol. 50, 4752–4759.
NRC, 2004. Air Quality Management in the United States, National Research Council. The Natiional Academies Press, Washington, DC.
Pusede, S.E., Duffey, K.C., Shusterman, A.A., Saleh, A., Laughner, J.L., Wooldridge, P.J., Zhang, Q., Parworth, C.L., Kim, H., Capps, S.L., Valin, L.C., Cappa, C.D., Fried, A., Walega, J., Nowak, J.B., Weinheimer, A.J., Hoff, R.M., Berkoff, T.A., Beyersdorf, A.J., Olson, J., Crawford, J.H., Cohen, R.C., 2016. On the effectiveness of nitrogen oxide reductions as a control over ammonium nitrate aerosol. Atmos. Chem. Phys. 16, 2575–2596.
Sacks, J.D., Lloyd, J.M., Zhu, Y., Anderton, J., Jang, C.J., Hubbell, B., Fann, N., 2018. The Environmental Benefits Mapping and Analysis Program – Community Edition (BenMAP–CE): a tool to estimate the health and economic benefits of reducing air pollution. Environ. Model. Softw 104, 118–129.
Shah, V., Jaeglé, L., Thornton, J.A., Lopez-Hilfiker, F.D., Lee, B.H., Schroder, J.C., Campuzano-Jost, P., Jimenez, J.L., Guo, H., Sullivan, A.P., Weber, R.J., Green, J.R., Fiddler, M.N., Bililign, S., Campos, T.L., Stell, M., Weinheimer, A.J., Montzka, D.D., Brown, S.S., 2018. Chemical feedbacks weaken the wintertime response of particulate sulfate and nitrate to emissions reductions over the eastern United States. Proc. Natl. Acad. Sci. Unit. States Am. 115, 8110–8115.
Shi, L.H., Zanobetti, A., Kloog, I., Coull, B.A., Koutrakis, P., Melly, S.J., Schwartz, J.D., 2016. Low-concentration PM2.5 and mortality: estimating acute and chronic effects in a population-based study. Environ. Health Perspect. 124, 46–52.
USEPA, 2007. Guidance on the Use of Models and Other Analyses for Demonstrating Attainment of Air Quality Goals for Ozone, PM2.5, and Regional Haze. U.S. EPA, Office of Air Quality Planning and Standards, Research Triangle Park, NC Available: https://www3.epa.gov/ttn/scram/guidance/guide/final-03-pm-rh-guidance.pdf.
USEPA, 2010. Quantitative Risk Assessment for Particulate Matter – Final Report. U.S. EPA, Office of Air Quality Planning and Standards, Research Triangle Park, NC EPA-452/R- 10-005. Available: http://www.epa.gov/ttn/naaqs/standards/pm/s_pm_2007_risk.html.
USEPA, 2014. Health Risk and Exposure Assessment for Ozone. Final Report. U.S. EPA, Office of Air Quality Planning and Standards, Research Triangle Park, NC EPA-452/R-14-004a. Available: https://www3.epa.gov/ttn/naaqs/standards/ozone/data/20140829healthrea.pdf.
USEPA, 2017. Bayesian Space-Time Downscaling Fusion Model (Downscaler) -Derived Estimates of Air Quality for 2013. U.S. Environmental Protection Agency, Office of Air Quality Planning and Standards, Research Triangle Park, NC EPA-450/R-17-001. Available: https://www.epa.gov/hesc/rsig-related-downloadable-data-files.
van Donkelaar, A., Martin, R.V., Spurr, R.J.D., Burnett, R.T., 2015. High-Resolution satellite-derived PM2.5 from optimal estimation and geographically weighted regression over North America. Environ. Sci. Technol. 49, 10482–10491.
Wang, M., Sampson, P.D., Hu, J.L., Kleeman, M., Keller, J.P., Olives, C., Szpiro, A.A., Vedal, S., Kaufman, J.D., 2016. Combining land-use regression and chemical transport modeling in a spatiotemporal geostatistical model for ozone and PM2.5. Environ. Sci. Technol. 50, 5111–5118.
Wang, Y., Hu, X., Chang, H., Waller, L., Belle, J., Liu, Y., 2018. A bayesian downscaler model to estimate daily PM2.5 levels in the conterminous US. Int. J. Environ. Res. Public Health 15, 1999.
Young, M.T., Bechle, M.J., Sampson, P.D., Szpiro, A.A., Marshall, J.D., Sheppard, L., Kaufman, J.D., 2016. Satellite-based NO2 and model validation in a national prediction model based on universal kriging and land-use regression. Environ. Sci. Technol. 50, 3686–3694.